Wave Phenomena

Adams, Jake
jake.adams@mail.utoronto.ca
1003847377

Jiang, Hansen
hansen.jiang@mail.utoronto.ca
1003192403

December 8, 2018

Introduction

The purpose of this experiment was to study the properties of two-dimensional waves by observing the behavior of water waves in a ripple tank.

Methods and Materials

- ripple tank
- light reflector
- ripple generator
- light source
- dippers
- attachments
- reflectors
- refractors
- barriers
- ruler
- measuring cup
- level
- data acquisition program

Experimental Procedure

To begin, the knobs on the feet of the ripple tank apparatus were adjusted until the tank was leveled. After confirming the state of the evacuation tube clamp to be in the closed position, approximately 800mL of tap water was added to the tank. The ripple generator was positioned over the midpoint of one side of the tank. With the plane wave dipper mounted on the generator, the height of the device was slightly adjusted until the dipper just barely touched the surface of the water and held equal contact over its entire length. In the other axis, the generator was corrected to be parallel to the wall of the tank it resided over.

For the first exercise, a long straight barrier was placed into the center of the tank at an angle to the generator; the water level in the tank was set to halfway up the barrier. Next, the frequency of the generator was set to 20Hz and amplitude set to less than half maximum. Utilizing both light source settings to accomplish the best viewing (STROBE and STEADY) of the pattern of plane waves, the angle of incidence and reflection were measured. This process was completed NUMBER times, each with the barrier at a different angle. Next, the straight barrier was replaced with a a curved barrier, positioned in front of the generator with the curve towards it. The reflected wave pattern was observed, and the focal distance and radius of the curve were estimated. The barrier was then turned 180 degrees and the same measurements were repeated.

In the second exercise, the same setup was used, except without any barrier in the tank. The frequency was set to 5Hz and the amplitude to less than half maximum. Then, the length of four wavelengths were recorded and then averaged to find an approximation for one wavelength. The process was repeated for five other frequencies. After, a similar process was performed, except the frequency was fixed and the water depth within the tank as varied between 2mm to 10mm. Using this data, wave speed was estimated at each depth.

Exercise 3 introduced the trapezoidal refractor into the tank setup. The triangular end was positioned towards the plane wave dipper and the water level was increased so that it exceeded the height of the refractor by a couple millimeters. With the frequency set to 15Hz, the refraction pattern was recorded, along with the angles of incidence and refraction.

For exercise 4, two straight barriers were placed in front of the plane wave dipper to from a 3cm slit. The generator was set to 20Hz and amplitude to half maximum, then the diffraction patter was observed. The angular spread of the circular waves moving outwards from the slit was estimated for five different slit widths.

In the final exercise, the plane wave dipper was replaced with two standard dippers. As before, the dippers were calibrated before experimentation to allow them to just barely make contact with the surface of the water. The frequency was set to 20Hz and amplitude to half maximum. The resulting pattern was then observed and the angles corresponding to each order of interference were measured. Then, process was repeated with the distance between the dippers varied. Finally, one dipper was set in opposition of phase, and the resulting pattern was observed.

Results

The first exercise attempted to form a straightforward relationship,

$$\theta = \theta' \tag{1}$$

with θ and θ' representing the incidence and reflection angles of the wavefront on the straight barrier. The correlation was formed, with the following results using random positions of the barrier.

Trial	θ ($^\circ$)	θ' ($^\circ$)	$\sigma_{\theta,\theta'}$ ($\pm^\circ$)	$\frac{\theta}{\theta'}$ (1 ± 10^{-4})
1	46.23	42.28	0.01	1.093 ± 4
2	31.95	28.14	0.01	1.135 ± 5
3	63.98	60.69	0.01	1.054 ± 2
4	32.29	32.99	0.01	0.9788 ± 4
5	20.45	16.89	0.01	1.211 ± 0.4
6	51.47	45.56	0.01	1.130 ± 3

Table 1: Comparing incidence and reflection angles in Exercise 1

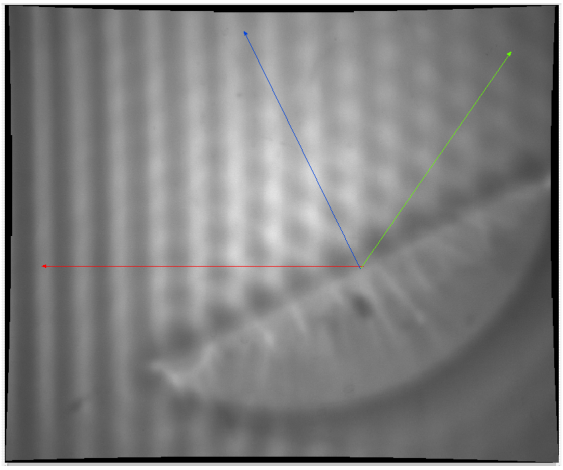

Figure 1: Reflection on a straight barrier

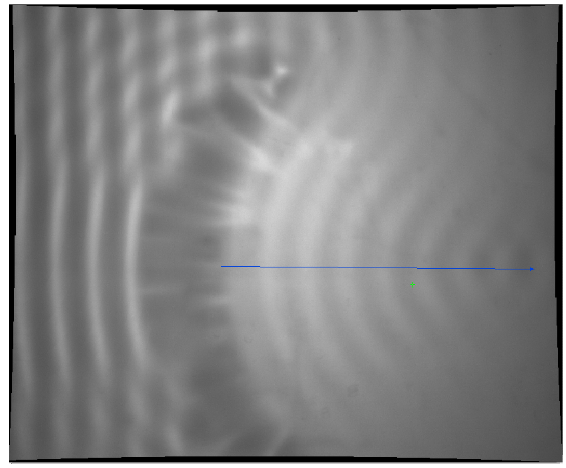

Figure 2: Focal distance of a curved barrier

The second part of the first exercise used properties of smoothly curved convex and concave ”mirrors” to measure characteristics such as focal distance, and radius of curvature, with the following results.

Type	f (cm)	C (cm)	σ_C ($\pm$cm)
Convex	8.61	17.22	0.02
Concave	3.19	6.38	0.02

Table 2: Comparing focal distances of convex and concave barriers

where f is the focal distance, $C = 2 \cdot f$ is the radius of curvature, σ_C is the error associated with C, and Type is the type of mirror the barrier acts as when oriented towards the wave the way it was at the time of recording.

The second exercise attempted to establish a relationship between the frequency f of the wave with its wavelength λ, by the equation

$$v = f\lambda \tag{2}$$

with v representing the speed of the wave. This relationship is expected to be linear, and when plotting λ_{AV} vs f, the relationship becomes

$$\lambda = v \cdot \frac{1}{f} \tag{3}$$

where frequency f scales reciprocally with the x-axis. Simply plotting the frequency of the waves vs the wavelengths yields $1/r$ correlation. Plotting the reciprocal of the frequency against the wavelength shows the expected linear trend of Equation 3. The slope of the linear regression is then v, which can be compared to the expected shallow water gravity wave value,

$$v = \sqrt{gd} \tag{4}$$

where $g = 9.81\frac{\mathrm{m}}{\mathrm{s}^2}$ is the acceleration due to near-surface Earth gravity, and d is the depth of the water in m.

The data recorded is visualized as follows.

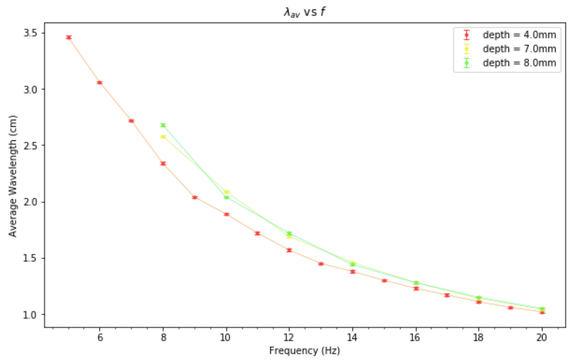

Figure 3: Many points at few depth differences, first sample

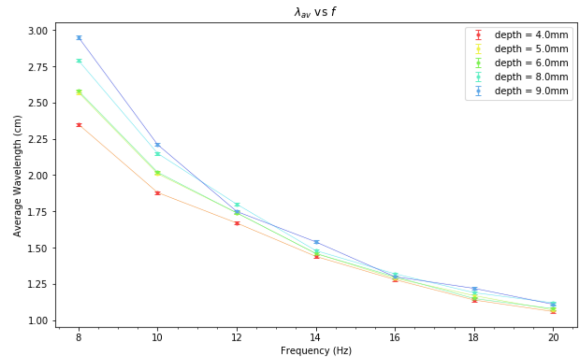

Figure 4: Fewer points at many depth differences, second sample

The first session consisted of the collection of every integer value of the frequency at a single depth level, to identify the relationship between the variables. The second session measured fewer values at five different depths. This data can be plotted by the linear fit as determined by Equation 3, and the value of v can be compared with that of Equation 4. In the following table, v is the value of the slope, and c is the intercept, which should ideally be 0, σ_v, σ_c are the corresponding errors, v_e is the expected speed by Equation 4, and χ^2_{red} is the goodness of fit associated with the linear fit, and 1 is the optimal value. The corresponding plots can be found on the following page.

Depth (mm)	v_e (m/s)	v (m/s)	σ_v ($\pm 10^{-3}$m/s)	c (mm)	σ_c ($\pm 10^{-4}$m)	χ^2_{red}	Figure
4	0.1981	0.1703	3	1.708	3	24.12	3
7	0.2620	0.2078	3	-0.1467	2	3.605	3
8	0.2801	0.2156	6	-0.6462	5	16.26	3
4	0.1981	0.1709	4	2.085	3	6.572	4
5	0.2215	0.1993	4	0.5597	3	6.891	4
6	0.2426	0.2009	4	0.4609	3	7.191	4
8	0.2801	0.2252	7	-0.7027	6	22.01	4
9	0.2971	0.2440	10	-1.839	10	57.80	4

Table 3: Optimized vs expected wave speeds for various water depths

Plotting Exercise 2b with v against λ, and v calculated by Equation 2, yields the following plots.

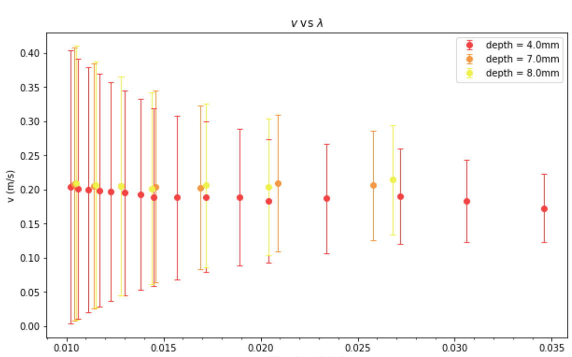

Figure 5: Wave speed vs λ, first set

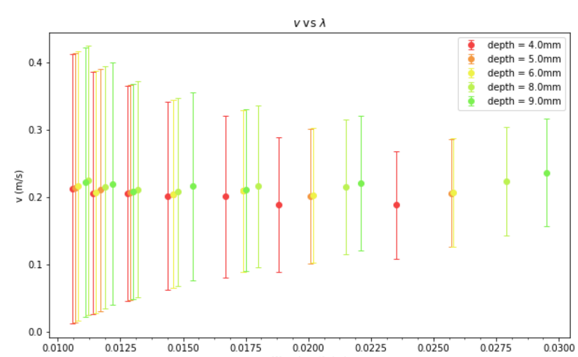

Figure 6: Wave speed vs λ, second set

The linear fits plotted against the data from Figures 3 and 4, with errors, are as follows.

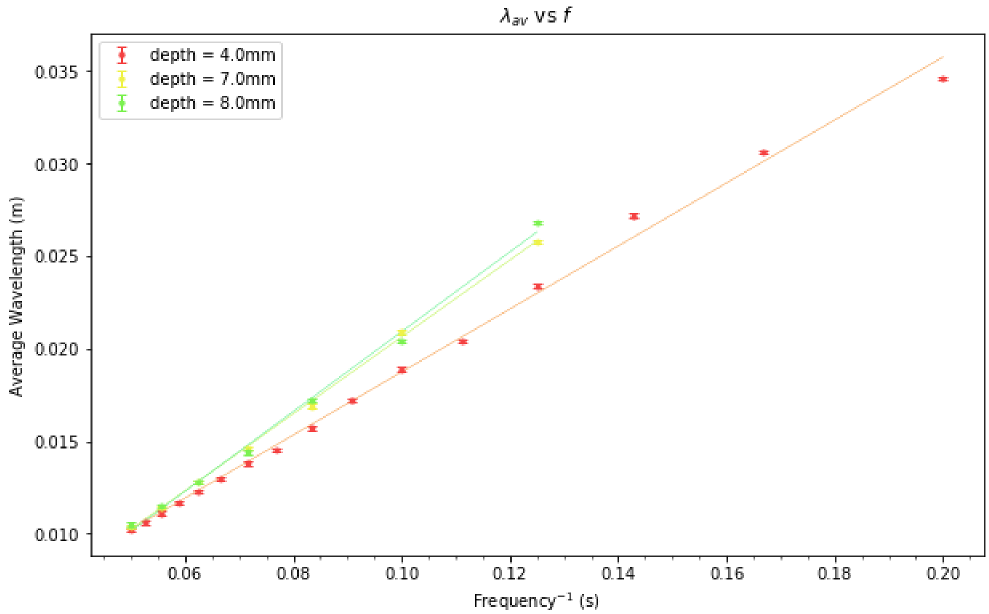

Figure 7: Linear regression for first data set

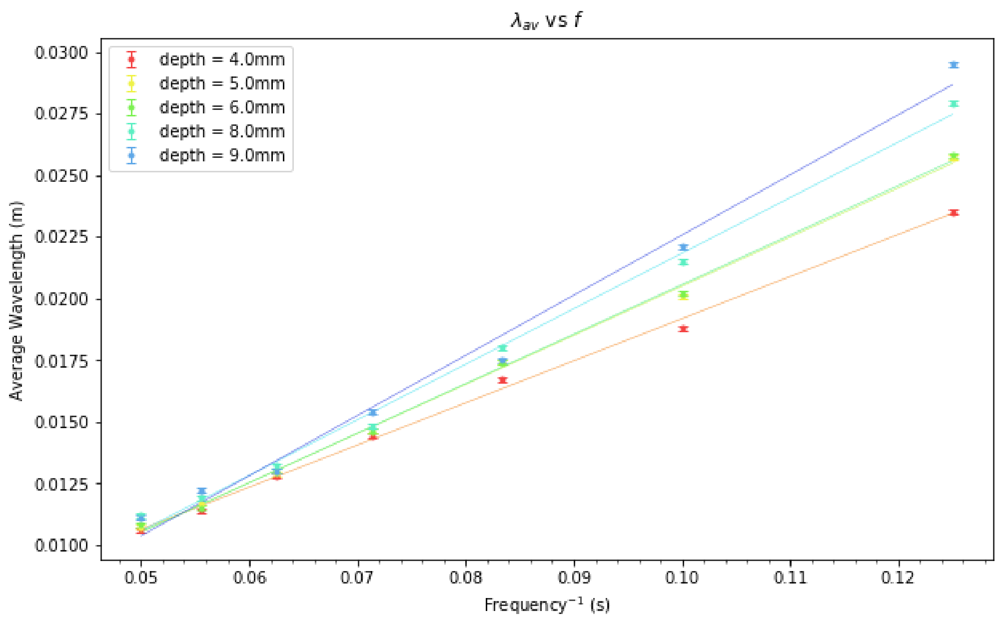

Figure 8: Linear regression for second data set

The third exercise attempted to demonstrate Snell's law, in the form

$$\frac{1}{v_1}\sin\theta_i = \frac{1}{v_2}\sin\theta_r \tag{5}$$

where v_1, v_2 are the velocities of the wave in two different media, and θ_i, θ_r are the incidence and refraction angles, respectively. This equation relates the angles of a wave as it passes through different media.

The observed images of Exercises 3 and 4 are as follows.

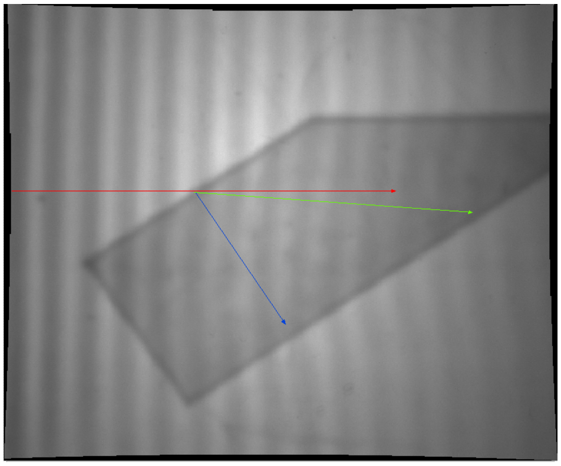

Figure 9: Refraction angles, Exercise 3

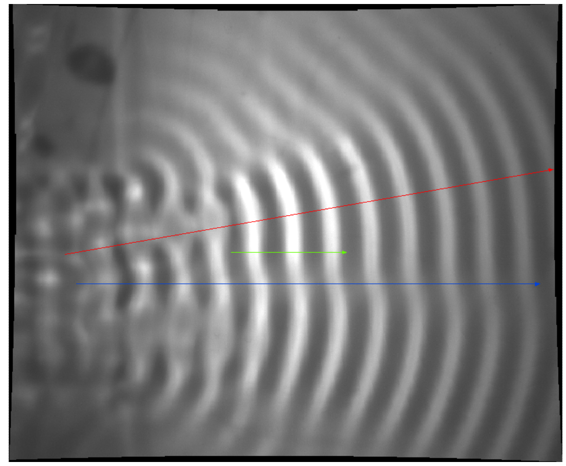

Figure 10: Single slit diffraction, Exercise 4

From the setup in Figure 9, the angles θ_i and θ_r were measured. With $f = 20.0Hz$ and measuring wavelength λ, the wave speed can be found by Equation 2. With this information, Equation 5 can be verified.

θ_i ($^\circ$)	θ_r ($^\circ$)	$\sigma_\theta(\pm^\circ)$	Eq. 5 LHS	Eq. 5 RHS
55.61	51.56	0.01	4.106	3.956

Table 4: Comparing angles of a wave as it travels through a different medium

The final two exercises concerned the circular waves generated by small dippers. The patterns formed can be seen in Figures 10 to 13.

Exercise 4 concerns diffraction patterns formed by a wave passing through a single slit. It attempts to verify the equation

$$a \sin\theta = \lambda \tag{6}$$

where a is the slit width, θ is the angular spread, and λ is the wavelength of the wave. The average wavelength was recorded to be $1.09 \pm 0.01cm$. Plotting the width of the angular spread against $1/a$ is as follows.

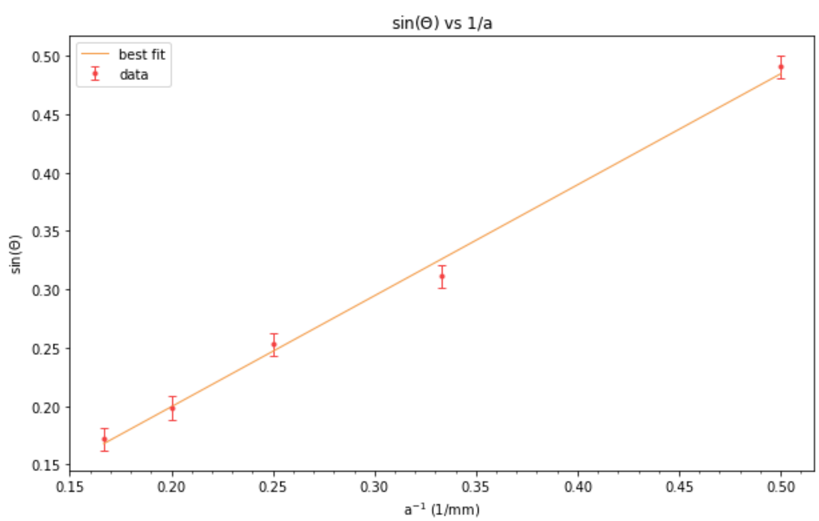

Figure 11: Width of spread vs slit width reciprocal, Exercise 4

From Equation 6, the slope of this plot is represented by λ, the wavelength, which was fitted to be $\lambda_{fit} = 0.9501 \pm 0.04$cm, which is not within one standard deviation of the measured average λ (but it is within four).

The fifth exercise concerned interference from two dipper sources, in attempting to verify the equation

$$A(\theta) = A_{max} \quad when \ \frac{kd\sin\theta}{2} = \frac{\pi d \sin\theta}{\lambda} = 0 \tag{7}$$

The observed patterns are as below.

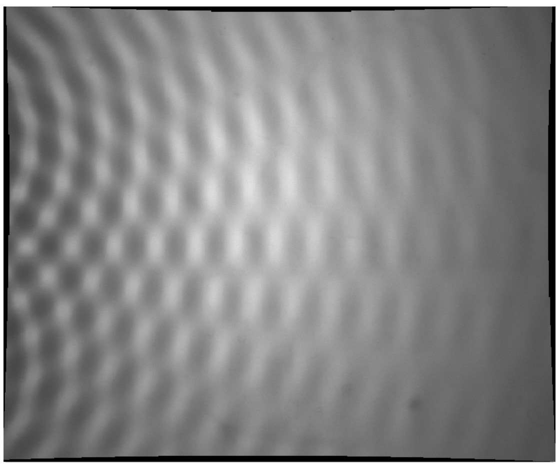

Figure 12: Out of phase interference, Exercise 5

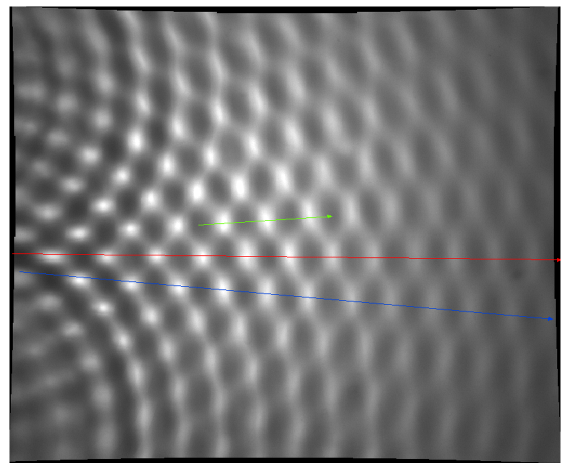

Figure 13: in phase interference, Exercise 5

With two dippers in phase, the interference pattern formed can be seen in Figure 13. When out of phase, the pattern can be seen in Figure 12. The stronger lines can be explained with constructive (in-phase) and destructive (out-of-phase) interference.

The recorded data is as follows.

Wavelength	$m = 1$ (°)	$m = 2$ (°)	$m = -1$ (°)	$m = -2$ (°)	d (cm)
1.14	8.69	16.38	7.57	14.87	6.5
1.23	4.35	10.13	4.39	9.74	10
1.37	2.77	4.58	2.65	5.05	15

Table 5: Comparing angles of various maxima at different separations

where each m is the angle corresponding to the m^{th} maximum in the pattern.

These angles occur at the maximum brightness between the "lines" as can be observed above, and correlate with Equation 7.

Discussion

The obvious advantage in using water waves to measure various characteristics and properties of general waves is the relative ease in observing them. Compared to visually invisible sound waves and light waves which can be detected as intensities, water waves allow for clear visualization of entire wavefronts moving and interacting with their environments.

These exercises proved to show various phenomena and equations describing waves, and some concerning only water waves. If the recorded values were not within their associated uncertainties of the expected values, the correlation and expected similarity is at least present.

In terms of uncertainty and error, the greatest source by far is human approximation. The accuracy and ability of the equipment to oscillate at the rate at which it does is more precise than human ability to approximate angles and determine the approximate beginnings and endings of wavelengths. Since the measurements were made by approximation, many were made in the effort of statistically eliminating misrepresentation errors. The uncertainties used in this lab are reading errors, based on the inherent fluctuations in the last digit of a measured value.

Conclusion

The ripple tank setup provides an incredibly resourceful and accurate model of some of the complex properties of two-dimensional wave patterns. From examining reflection, refraction, diffraction, and interference in the tank, the collected data can be used to confirm wave equations and theorem.